

Aerodynamic Performance of Wing with Winglet at Low Reynolds Number

D. Raj Kumar ME^[1] S. Arun Kumar^[2] S. Chinnaiyan^[3] P. Priyadharshan^[4] C. Aravindh^[5]

Professor, Bachelor of Engineering in Aeronautical, Paavai Engineering College, Namakkal, India^[1]

Student, Bachelor of Engineering in Aeronautical, Paavai Engineering College, Namakkal, India^{[2]-[5]}

Abstract: Administrative common aeronautics offices are pushing airplane producers and administrators to improve airplane proficiency by lessening fuel utilization, cutting carbon dioxide CO₂ and nitrogen oxide NO_x emanations, and bringing down the apparent outer commotion. The above problems can't be rectified fully but we can ably minimize the fuel consumption, so automatically carbon dioxide and nitrogen oxide will be reduced. The best solution is to decrease the lift induced drag in the way of changing the cant angle of the winglet. So, we design a straight wing and with different sweep angle using the Catia V5 after creating these wings and we go to the CFD for analyzing the wings at certain condition. Using Winglet, the aerodynamic performance will be investigated in Low Reynolds No regime. Winglet configuration will be varied in terms of sweep back angle and cant angle. Best configuration will be optimized.

Keyword - Aerodynamic performance, Cant angle, lift induced drag, low Reynolds number, Winglet

I. INTRODUCTION

On the planet such countless airplanes are flying in the sky which was planned by the great plan engineer who's know the essentials of the airplane. On the yield of newton third law "For each activity there is an equivalent and inverse response" from this, for each power are go about as a twin. From above the statement wherever the forward(thrust) force occurs there is equal or less backward(drag)force are formed. During the design of aircraft one of the major challenges is drag. We choose to reduce the one of the major drags is life induced drag for our project which set up by the pressure difference occurs on each side of the wing tip of the aircraft. On the surrender of general thermodynamic law is any place the high temperature district happens it will arrive at the low temperature area to remunerate the change of the temperature, from this the base surface of the wing have a high-pressure locale and the top surface of the wing have a low-pressure district, so because of this pressing factor distinction, in the lower part of high pressing factor is burdening to move to the low-constrain area to balance out the awkwardness of the pressing factor. During the give the high-compel area to low-pressure district is in the shape like circle, so the continuation of this interaction it's anything but a vortex. In view of this vortex the downwash will framed and interface with the neighbor relative smooth out progression of air so relative stream will be diverted. Because of this vortex and downwash, the presentation of the airplane will be diminishing and the fuel utilization is increment to make a push for pushing the airplane ahead. In any case, we can't stay away from this haul completely so we can lessen the effect of this drag in the method of render the cant point of the winglet to improve execution for the airplane.

II. DESIGN PROCESS

Before going to design a wing, we choose the best suitable airfoil for that wing because airfoil is the most efficient thing for the wing. While choosing the airfoil the lift/drag ratio is high so that only the better performance will be achieved. After choosing the airfoil, the Design parameter is must important to achieve the performance.

Design of wing with winglet: A rectangular wing plan has been designed and we coupled the winglet to the rectangle wing in the angle of 5°, 10° and 15° using the airfoil NACA 4415 using Catia V5 software with the surface modelling option.

Parameters for wing

Span of wing	0.9m
Root chord	0.1125m
Tip chord	0.023848
Sweep angle	5, 10, 15 degrees

Steps involved in wing design

Using Catia v5 and surface modelling option the wing can be created.

First, we import airfoil into coordinates and using spline option we can create airfoil for the wing.

After creating airfoil using translate option, we can move airfoil to next end.

For creating winglet, we need to scale the tip airfoil and using rotating option we can change the angle of wing let.

Now using multiple-surface option can generate complete wing design

Design of Fluid Domain

Parameters for Fluid Domain

Radius of domain 1.4m

Length of domain 2.25m

Steps Involved in Fluid Domain

After designing wing, we need to import our model to design-modular.

Creating C-domain using sketching option first need to create arc using arc-centre option and line option.

After creating sketch, we need to extrude sketch and use add frozen option.

Use Boolean option to make it as one fluid domain.

Meshing Process

After created the fluid domain, Now the straight wing and the different angle of wing with winglet are place inside of the fluid domain for mesh the straight wing and wing with winglet. An unstructured Mesh is generated in the C-domain using ICM- CFD for both wing and the fluid domain.

Steps Involved in Meshing

For generating mesh ICMCFD is used we have created unstructured mesh for both wing and fluid domain.

Also created prism layer for wing.

Determinant value of mesh is 1 and skewness of wing is also lesser than 0.9.

After doing mesh convergence we came with 2171839 elements.

And we used total of 12 prism layers over the wing.

III. NUMERICAL PROCEDURE

The fundamental strategy continued in this investigation is the mathematical arrangement of Reynolds-Averaged three-dimensional Navier-Stokes conditions with a disturbance conclusion inside a rocket spout with infusion with the assistance of a business CFD bundle, called FLUENT®. What's more, a test arrangement for the virus stream trial of SITVC pointing CFD approval was wanted to be set up, the design of trial arrangement was drawn, basic equipment was chosen and primer testing without infusion was refined utilizing blower framework, spout and Scanivalve framework. Anyway because of the absence of subsidizing the continuation of this examination was cut. The itemized depiction of the exploratory arrangement is referenced in Appendix E. Accordingly, this examination in the end includes just the mathematical part generally.

Governing Equations

The Navier-Stokes equation for the compressible, viscous flow is numerically solved for the analysis of hypersonic flow in the three ramp inlets. The differential form of the Navier-stokes equation is given below as continuity, momentum, and energy equation.

Continuity equation

$$\frac{\partial \rho}{\partial t} + \frac{\partial}{\partial x_k} (\rho U_k) = 0 \quad k=1,2,3 \tag{3.1}$$

From the equation of momentum

$$\frac{\partial}{\partial t} (\rho u_i) + \frac{\partial}{\partial x_k} (\rho u_i u_k) + \frac{\partial p}{\partial x_i} = \frac{\partial (\tau_{ik})}{\partial x_i} \quad i, k = 1, 2, 3 \tag{3.2}$$

Where ρ - Density u_i - Velocity components p - Pressure

Turbulent shear stress is defined as

$$\tau_{ik} = \mu \left(\frac{\partial u_i}{\partial x_k} + \frac{\partial u_k}{\partial x_i} \right) \tag{3.4}$$

$\mu = \mu_l + \mu_t$ is the total viscosity;

μ_l - Laminar viscosity μ_t - Turbulent viscosity

Laminar viscosity (μ_l) is calculated from Sutherland law as

$$\mu_l = \mu_{ref} \left(\frac{T}{T_{ref}} \right)^{\frac{3}{2}} \left(\frac{T_{ref} + S}{T + S} \right) \tag{3.5}$$

Where T is the temperature and μ_{ref} , T_{ref} and S have known coefficients.

In swirl thickness models, the pressure tensor is communicated as a component of tempestuous consistency (μ_t). In view of dimensional investigation, barely any factors (k, ϵ, ω) is characterized as given beneath,

Turbulent kinetic energy k,

$$k = \overline{u'_i u'_i} / 2 \tag{3.6}$$

Turbulent dissipation rate ϵ ,

$$\varepsilon = \nu \overline{\frac{\partial u'_i}{\partial x_j} \left(\frac{\partial u'_i}{\partial x_j} + \frac{\partial u'_j}{\partial x_i} \right)} \tag{3.7}$$

Specific dissipation rate ω ,

$$\omega = \varepsilon/k \tag{3.8}$$

The turbulent viscosity μ_t is calculated as

$$\mu_t = c_\mu \frac{\rho k^2}{\varepsilon} \tag{3.9}$$

The heat flux q_k is calculated as

$$q_k = -\lambda \left(\frac{\partial T}{\partial x_k} \right) \tag{3.10}$$

λ is the thermal conductivity.

k- ω Turbulence Model

The turbulent viscosity is determined as an element of k and ω .

$$\mu_t = f \left(\frac{\rho k}{\omega} \right) \tag{3.11}$$

Turbulent kinetic energy (k) equation:

$$\frac{\partial}{\partial t} (\rho k) + \frac{\partial}{\partial x_i} (\rho k u_i) = \frac{\partial}{\partial x_j} \left(\Gamma_k \frac{\partial k}{\partial x_j} \right) + G_k - Y_k \tag{3.12}$$

Specific dissipation rate (ω) equation:

$$\frac{\partial}{\partial t} (\rho \omega) + \frac{\partial}{\partial x_i} (\rho \omega u_i) = \frac{\partial}{\partial x_j} \left(\Gamma_\omega \frac{\partial \omega}{\partial x_j} \right) + G_\omega - Y_\omega \tag{3.13}$$

Where G_k , Y_k , Γ_k and G_ω , Y_ω , Γ_ω are the creation, dispersal and dissemination terms of the k and ω conditions separately.

IV. FIGURES AND TABLES

Wing With Winglet

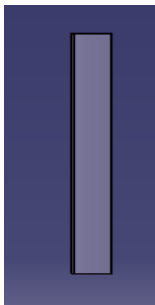


Fig 1 Straight wing

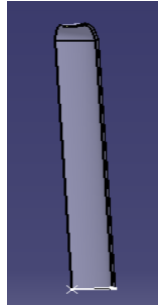


Fig 2 sweep with 5°

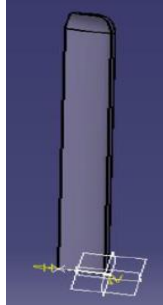


Fig 3 sweep with 10°

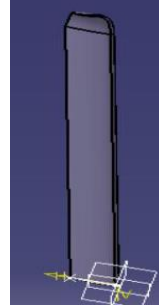


Fig 4 sweep with 15°

Fluid Domain

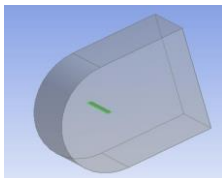


Fig 5 Fluid domain with straight wing

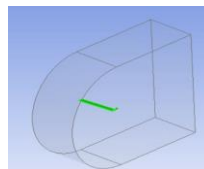


Fig 6 Fluid domain with winglet

Fluent Setup

Table 1 Fluent set up for meshing

After creating mesh import mesh file to fluent and set the boundary conditions. Condition	Steady
Domain	Air
Inlet	Velocity, Temperature
Outlet	Pressure outlet
wall	Free slip wall
Symmetry	Symmetry
Wing	Wall
Velocity	30m/s
Atmospheric pressure	1 atm
Method	k-epsilon
Solver	Coupled with second order

Prism Layer Over Wing



Fig 7 Illustration of unstructured mesh created on the Fluid domain and the Airfoil

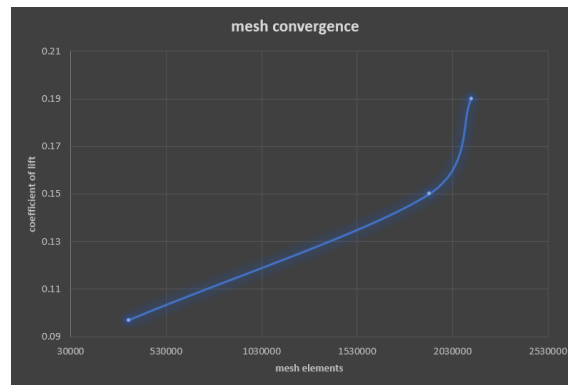


Fig 8 Mesh Convergence Study

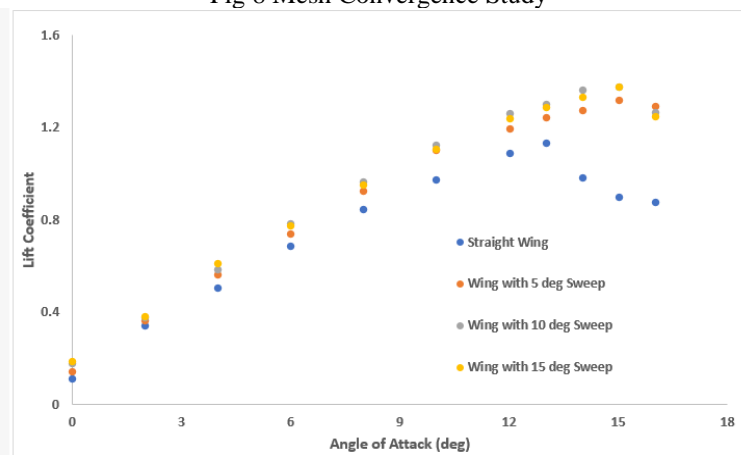


Fig 9 C_L vs Alpha

The above Figure illustrates the variation in C_L with changes in angle of attack (AOA) for the wing with and without winglet cases. It is evident from the figure that the C_L has determinantal effect due to including a winglet at the tip of the wing. Also, there is appreciable increase in maximum C_L while incorporating sweep back angle to the winglet.

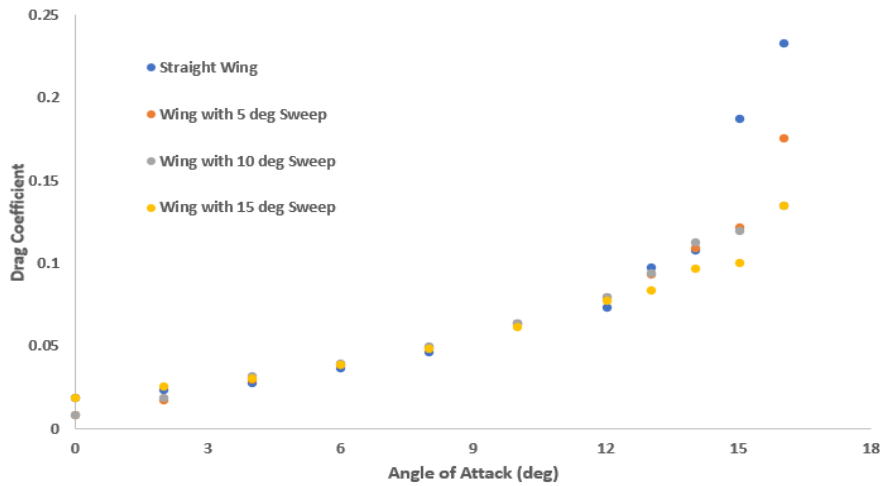


Fig 10 C_D vs Alpha

The above figure illustrates the changes in drag coefficient (C_D) for the different AOA while incorporating winglet to the plain wing and also varying the sweep back angle for the winglet. In the very AOA, the effect is minimal because of including winglet and also the sweepback angle to the winglet. At the same time, the effect predominantly reduces the C_D at the higher angle of attack.

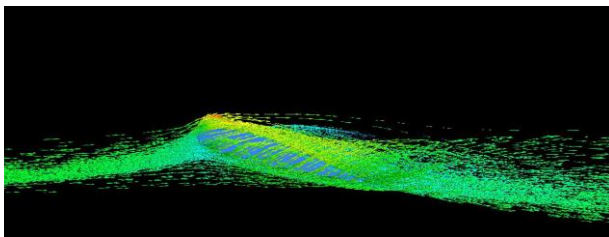


Fig 11 Straight wing

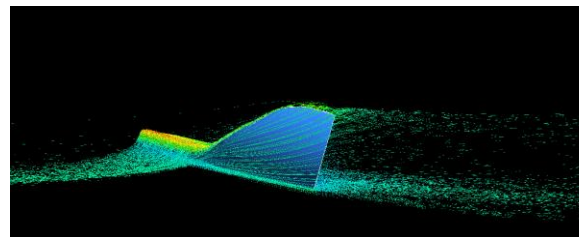


Fig 12 Sweep with 5°

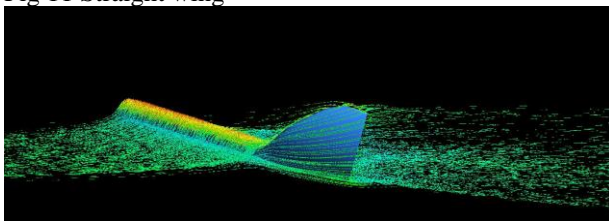


Fig 13 Sweep with 10°

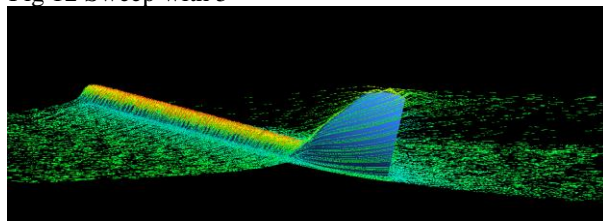


Fig 14 Sweep with 15°

V. CONCLUSION

The fuel efficiency, in turn the aerodynamic efficiency of flying vehicles is important in the present day competitive economic world. An investigation has been carried out for increasing the aerodynamic efficiency (L/D) of the wing by introducing winglet at the tip of the straight wing and also the same effect has been studied further by introducing sweepback angle to the same winglet. This phenomenon has been examined by numerically for a semi-wing configuration at low Reynolds number by solving RANS equations with turbulence model. Three-dimensional wing model has been generated using CATIA modelling software. Numerical simulation has been carried in the commercial CFD Package. The numerical simulation results clearly shows that the C_L increases and C_D decreases while incorporating winglets to the straight wing and also further improvement in these quantities has been for incorporating sweepback angle to the winglet. Also, the variation in aerodynamic efficiency parameter (C_L/C_D) has determinantal effect due to the winglets and also winglet sweepback angle when compared to the straight wing. This effect is well supported and well visualized with vortex pattern seen in the wing tip portions.



REFERENCE

- [1] Aerodynamics, Aeronautics, and Flight Mechanics, Second Edition Barnes W. McCormick, Pennsylvania State University 57506-2
- [2] Guerrero J, Sanguineti M, Wittkowski K (2018) CFD study of the impact of variable cant angle winglets on total drag reduction. Aerospace 5(4):126
- [3] Bennet, D., Dec. 2001, "The Wing Grid: A New Approach to Reducing Induced Drag," Final Report 16.662.
- [4] Performance analysis of a wing with multiple winglets M. Smith, N. KomerathR, AmesO. Wong and J. Pearson Published Online:22 Aug 2012
- [5] Performance comparison of different winglets by CFD AIP Conference Proceedings 2121, 060006 (2019)
- [6] Yin K-S (2017) A study of carbon dioxide emissions reduction opportunities for airlines on Australian international routes. Ph.D. thesis, University of Queensland
- [7] Pankonien AM (2015) Smart material wing morphing for unmanned aerial vehicles. Ph.D. thesis, University of Michigan.